DMD Fast Forward. Published on June 26, 2020 as DOI: 10.1124/dmd.120.091041
This article has not been copyedited and formatted. The final version may differ from this version.

Modulation of Major Human Liver Microsomal Cytochromes P450 by Component Alkaloids of Goldenseal: Time-Dependent Inhibition and Allosteric Effects

Matthew G. McDonald, Dan-Dan Tian[1], Kenneth E. Thummel, Mary F. Paine, Allan E. Rettie

Departments of Medicinal Chemistry (MGM, AER) and Pharmaceutics (KET), School of Pharmacy, University of Washington, Seattle, WA, 98195; Department of Pharmaceutical Sciences (DDT, MFP), College of Pharmacy and Pharmaceutical Sciences, Washington State University, Spokane, WA, 99202; Center of Excellence for Natural Product Drug Interaction Research (KET, MFP, AER)

Running Title: Complex Effects of Goldenseal Alkaloids on CYPs

Corresponding author:

Matthew G. McDonald, Ph.D.

Department of Medicinal Chemistry

University of Washington, Box 357610

1959 NE Pacific, Seattle WA 98195

Telephone: (206) 384-3386

Fax: (206) 685-3252

Email: mcmatt@uw.edu

Number of:

Text pages: 44

Tables: 6

Figures: 6

References: 39

Words in Abstract: 250

Words in Introduction: 734

Words in Discussion: 1701

Abbreviations: AUC, area under the plasma concentration versus time curve; CYP, cytochrome P450; $f_{u,HLM}$, fraction unbound in human liver microsomes; $f_{u,p}$, fraction unbound in plasma; GSE, goldenseal extract; HLMs, human liver microsomes; $I_{max,u}$, maximum unbound plasma concentration; KP_i, potassium phosphate; MDZ, midazolam; MI, metabolic intermediate; NP, natural product; PBPK, physiologically-based pharmacokinetic; TDI, time-dependent inhibition

ABSTRACT

Botanical and other natural products (NPs) are often co-consumed with prescription medications, presenting a risk for cytochrome P450 (CYP)-mediated NP-drug interactions. The NP goldenseal (*Hydrastis canadensis*) has exhibited anti-microbial activities in vitro attributed to isoquinoline alkaloids contained in the plant, primarily berberine, (-)-β-hydrastine and to a lesser extent, hydrastinine. These alkaloids contain methylenedioxyphenyl rings, structural alerts with potential to inactivate CYPs through formation of metabolic intermediate complexes. Time-dependent inhibition experiments were conducted to evaluate their ability to inhibit major CYP activities in human liver microsomes using a cocktail of isozyme-specific substrate probes. Berberine inhibited CYP2D6 (dextromethorphan *O*-demethylation; K_I = 2.7 μM, k_{inact} = 0.065 min^{-1}) and CYP3A4/5 (midazolam 1'-hydroxylation; K_I = 14.8 μM, k_{inact} = 0.019 min^{-1}); (-)-β-hydrastine inhibited CYP2C9 (diclofenac 4'-hydroxylation; K_I = 49 μM, k_{inact} = 0.036 min^{-1}), CYP2D6 (K_I > 250 μM, k_{inact} > 0.06 min^{-1}) and CYP3A4/5 (K_I = 28 μM, k_{inact} = 0.056 min^{-1}); and hydrastinine inhibited CYP2D6 (K_I = 37 μM, k_{inact} = 0.049 min^{-1}) activity. Berberine additionally exhibited allosteric effects on midazolam hydroxylation, showing both positive and negative heterotropic cooperativity. Experiments with recombinant isozymes showed that berberine activated midazolam 1'-hydroxylation by CYP3A5, lowering $K_{m(app)}$, but showed mixed inhibition and negative cooperativity towards this reaction when catalyzed by CYP3A4. Berberine inactivated CYP3A4 at a much faster rate than CYP3A5 and was a non-competitive inhibitor of midazolam 4-hydroxylation by CYP3A4 but a strong mixed inhibitor of the CYP3A5 catalyzed reaction. These complex kinetics should be considered when extrapolating the risk for NP-drug interactions involving goldenseal.

SIGNIFICANCE STATEMENT

Robust kinetic parameters were determined for the reversible and time-dependent inhibition of CYP2C9, CYP2D6 and CYP3A4/5 activities in HLMs by major component isoquinoline alkaloids contained in the botanical natural product (NP) goldenseal. The alkaloid berberine also exhibited opposing, isozyme-specific, allosteric effects on midazolam hydroxylation mediated by recombinant CYP3A4 (inhibition) and CYP3A5 (activation). These data will inform the development of a physiologically-based pharmacokinetic model that can be used to predict potential clinically relevant goldenseal-drug interactions.

INTRODUCTION

Botanical natural products (NPs) include herbal and other dietary supplements (Paine and Roe, 2018). Many NPs occupy a growing niche in the contemporary health care market, presenting unique challenges in the context of concomitant drug therapy. Such challenges are due partly to a lack of product regulation and standardization, as well as the fact that plant extracts often contain a complex mixture of constituents that can vary substantially in both content and concentration depending on the preparation (Paine et al., 2018; Kellogg et al., 2019). Although up to 25% of adults report taking a dietary supplement with a prescription medication (Asher et al., 2017), there is a paucity of literature data examining potential NP-drug interactions for even widely used NPs.

Goldenseal (*Hydrastis canadensis* L. (Ranunculaceae)), a plant indigenous to southeastern Canada and the northeastern United States, is used to self-treat a wide spectrum of maladies, including the common cold, upper respiratory tract infections, and gastrointestinal and menstrual disorders. Goldenseal produces a variety of isoquinoline alkaloids (Figure 1A) that convey anti-microbial activity in vitro. The highest content alkaloids in goldenseal are berberine and (-)-β-hydrastine. The plant also contains a number of minor alkaloids, including hydrastinine, whose concentration in commercial extracts is highly dependent on the method of preparation (Weber et al., 2003; Ettefagh et al., 2011; Hermann and von Richter, 2012). Goldenseal appears unique among hydrastine-containing plants in that it produces only the (-)-enantiomer, whereas other plants produce primarily (+)-β-hydrastine (Gupta et al., 2015).

Several clinical studies have highlighted the potential for goldenseal extracts (GSEs) to precipitate NP-drug interactions by inhibiting cytochrome P450 (CYP) enzymes. Pre-treatment of human volunteers with a GSE (~1 g po 3x daily for 14 or 28 days) significantly inhibited both CYP2D6 and CYP3A4/5 activities (40-50% decrease in metabolite-to-parent ratios) and had negligible effects on CYP2E1 and CYP1A2 activities (Gurley et al., 2005; Gurley et al., 2008). Berberine (200 mg po 3x daily for 12 days) also inhibited CYP3A4/5-mediated cyclosporin A clearance (34.5% increase in AUC) in renal transplant recipients (Wu et al., 2005). Finally, berberine pre-treatment (300 mg po 3x daily for 14

days) followed by administration of an oral cocktail of CYP substrate probes resulted in a 10-fold, two-fold, and 1.6-fold increase in the parent-to-metabolite ratio for dextromethorphan (CYP2D6), losartan (CYP2C9), and midazolam (MDZ; CYP3A4/5), respectively (Guo et al., 2012).

In vitro experiments have evaluated the ability of GSE and/or one of the major alkaloids to reversibly inhibit human liver CYPs. One GSE exhibited the lowest IC_{50} (0.03% of full extract) for inhibition of CYP3A4 activity among 21 herbal extracts tested (Budzinski et al., 2000), and other studies reported strong inhibition (>50%) by a GSE of CYP3A4 and CYP2D6 activities. There are conflicting reports as to whether goldenseal inhibits CYP1A2, 2C9, 2C19 or 2E1 activities in vitro. Berberine generally has been shown to be a weak to moderate inhibitor of the CYP1As, as well as CYPs 2C8, 2D6, 2E1 and 3A4, and (-)-β-hydrastine to be a weak to moderate inhibitor of 2C8, 2C9, 2D6, 2E1 and 3A4 (Chatterjee and Franklin, 2003; Foster et al., 2003; Etheridge et al., 2007; Raner et al., 2007; Lo et al., 2013)

Two studies have evaluated the potential for goldenseal alkaloids to inactivate CYPs. Berberine exhibited time-dependent inhibition (TDI) of CYPs 2D6 and 3A4 (Zhao et al., 2015), while (-)-β-hydrastine showed TDI of CYP3A4 (Chatterjee and Franklin, 2003). Although both studies presented evidence for inactivation of specific CYPs by berberine and/or (-)-β-hydrastine, the reported inactivation kinetic parameters were approximations.

The objective of the present study was to define fully the mode and kinetics of inhibition of the major liver CYPs 2C9, 2D6 and 3A4/5 by the two major GSE component alkaloids, berberine and (-)-β-hydrastine, and the minor alkaloid, hydrastinine, which appears to be the third most abundant alkaloid present in some commercial extracts (Chatterjee and Franklin, 2003; Weber et al., 2003). Through comprehensive kinetic studies, robust parameters were recovered for both the reversible inhibition and TDI of CYPs 2C9, 2D6 and 3A4/5 by these three alkaloids. A comprehensive analysis of the unique kinetic allosteric interactions of berberine with CYP3A4 and CYP3A5 provided further insight into these

complex NP-drug interactions. The kinetic parameters generated can be used to develop physiologically-based pharmacokinetic (PBPK) models to predict the risk of goldenseal-drug interactions involving susceptible object drugs, aid in the design of clinical interaction studies, and help inform clinicians and consumers about managing these potentially adverse NP-drug interactions.

DMD Fast Forward. Published on June 26, 2020 as DOI: 10.1124/dmd.120.091041
This article has not been copyedited and formatted. The final version may differ from this version.

MATERIALS AND METHODS

General Reagents.

MDZ and 1'-OH-MDZ were obtained as 1 mg/mL and 100 μg/mL methanolic solutions, respectively, from Cerilliant (Round Rock, TX). Diclofenac sodium salt, berberine chloride, 1'-OH-MDZ-d_4, dextrorphan tartrate, dextrorphan tartrate-d_3 and 4'-hydroxydiclofenac-d_4 were purchased from Toronto Research Chemicals, Inc. (North York, ON); dextromethorphan was procured from LKT Laboratories, Inc. (St. Paul, MN). Hydrastinine, (-)-β-hydrastine, 4-OH-MDZ and all other chemicals were obtained from Sigma Aldrich Chemical Co. (St. Louis, MO). All inhibitors and substrates tested in these studies were deemed to be ≥ 95% pure. Solvents were purchased from J.T. Baker, Inc. (Phillipsburg, N.J.) or Fischer Scientific (Springfield, N.J.). Recombinant CYP3A4 and CYP3A5 Supersomes™, co-expressed in insect cells with cytochrome P450 oxido-reductase and cytochrome b_5, were purchased from Corning Life Sciences, Inc. (Corning, N.Y.). Pooled human liver microsomes (HLMs) of mixed gender were either prepared in-house from eight individual livers as reported previously (Sadeque et al., 1992; McDonald et al., 2015) or were purchased from Corning Life Sciences (Ultrapool HLM150) specifically for use in the berberine-MDZ allosterism experiments.

IC_{50} Shift Experiments for the Inhibition of CYP Activity by Berberine, (-)-β-Hydrastine or Hydrastinine.

Substrate cocktail assay. IC_{50} shift experiments were carried out using a validated substrate cocktail method (McDonald et al., 2015). Wells 1-24 and 25-48 of a 96-well plate contained identical solutions of inhibitor (added from 12 different 200x concentrated stock solutions, yielding final incubation inhibitor concentrations ranging from 0 to 500 μM), and pooled HLMs (final concentration, 0.25 mg/mL microsomal protein) in 100 mM KP_i buffer, pH 7.4. After a three-minute equilibration at 37°C/50 rpm in a water bath, 2.5 μL of NADPH stock (wells 1-24; final concentration,1 mM) or buffer without NADPH (wells 25-48) were added; final incubation volumes were 250 μL. The plate was incubated at 37°C for 30

minutes, then 196 μL were removed from each well and added to a second plate containing 2 μL of a 100x concentrated 3-substrate cocktail stock (prepared with 50% aqueous methanol; final concentrations: 4 μM diclofenac, 4 μM dextromethorphan and 2 μM MDZ) per well, plus 2 μL of either buffer alone (wells 1-24) or buffer with NADPH (1 mM final concentration, wells 25-48). This plate was incubated for 5 minutes at 37°C prior to quenching with 20 μL of ice cold 15% aqueous $ZnSO_4$. Ten pmols each of 1'-OH-MDZ-d_4 and dextrorphan-d_3 and 20 pmols of 4'-hydroxydiclofenac-d_4 were added as internal standards, then precipitates were removed by centrifugation and the supernatants analyzed by LC-MS/MS (described below).

MDZ assay. These experiments utilized the same methodology outlined above for the cocktail assay with the following exceptions: 1) either CYP3A4 or CYP3A5 Supersomes™ (3 pmols per incubation reaction) were substituted for HLMs as the enzyme source; 2) rather than using a substrate cocktail solution, a 100x concentrated stock solution containing MDZ (final substrate concentration of either 2 μM for the (-)-β-hydrastine experiments or 20 μM for the berberine experiments) was added to the second 96-well plate; and 3) 1'-OH-MDZ-d_4 (10 pmols) was added to each reaction product as internal standard.

LC-MS/MS Protocol. LC-MS/MS analysis was conducted with a Waters Xevo TQ-S Tandem Quadrupole Mass Spectrometer (Waters Co., Milford, MA) coupled to an ACQUITY Ultra Performance LC™ (UPLC™) System with an integral autoinjector (Waters). The Xevo was operated in ESI^+ mode at a source temperature of 150°C and a desolvation temperature of 350°C. The following mass transitions were monitored in separate ion channels for the substrate cocktail assay: *m/z* 258 → 157 (dextrorphan-d_0), *m/z* 261 → 157 (dextrorphan-d_3), *m/z* 312 → 230 (4'-hydroxydiclofenac-d_0), *m/z* 316 → 234 (4'-hydroxydiclofenac-d_4), *m/z* 342 → 324 (1'-OH-MDZ-d_0) and *m/z* 346 → 328 (1'-OH-MDZ-d_4) at cone voltages of 25, 23 and 30 V and collision energies of 35, 33 and 35 eV for dextrorphan, 4'-hydroxydiclofenac and 1'-OH-MDZ, respectively.

Metabolites from the substrate cocktail incubations were separated on a Shimadzu Shim-Pack XR-ODS, 2.2 μ, 2.0 x 75 mm LC column (Shimadzu Scientific, Colombia, MD) using a binary solvent gradient (solvent A = 0.1% aqueous formic acid and solvent B = methanol) with a constant flow rate of 0.35 mL/min and a column temperature of 50°C. From 0 to 1 minute, solvent was set at 20% B and increased linearly to 95% B from 1 to 5 minutes, which was maintained for 0.5 minutes and then re-equilibrated to 5% B over 0.2 minutes. Metabolites were quantified by comparison of their peak area ratios (relative to the 4'-hydroxydiclofenac-d_4, 1'-OH-MDZ-d_4 or dextrorphan-d_3 peak areas) to calibration curves, prepared with commercially obtained metabolite standards, using linear regression analysis. Limits of quantitation for 4'-hydroxydiclofenac, 1'-OH-MDZ and dextrorphan were, respectively, 3, 10 and 3 fmols of metabolite injected on the column.

Cytochrome P450 Kinetic Inactivation Experiments

Substrate cocktail assay: Incubations were carried out in 1.2-mL sample tubes for each of six inhibitor concentrations (added from 200x concentrated methanolic stock solutions to yield final concentrations ranging from 0 to 50 μM for berberine or 0 to 500 μM for (-)-β-hydrastine and hydrastinine). Each incubation contained 0.25 mg/mL pooled HLMs in 100 mM KP_i buffer, pH 7.4. The tubes were equilibrated at 37°C/50 rpm for three minutes in a water bath prior to initiating the reactions with NADPH (1 mM in 1.1 mL final volume). At 0, 5, 10, 15 and 20 minutes, 198-μL aliquots were removed and added to 2 μL of a 100x concentrated substrate cocktail stock solution (in 50% aqueous methanol) to yield final concentrations of 40 μM diclofenac, 40 μM dextromethorphan and 20 μM MDZ. The substrate reactions were incubated for 5 minutes at 37°C/50 rpm then quenched with 20 μL of 15% aqueous $ZnSO_4$, after which 10 pmols each of 1'-OH-MDZ-d_4 and dextrorphan-d_3 and 20 pmols of 4'-hydroxydiclofenac-d_4 were added as internal standards. Protein precipitate was removed by centrifugation, and metabolites within the supernatants were quantified by LC-MS/MS analysis. The LC-MS/MS protocol used for these experiments was identical to that used in the IC_{50} shift experiments (described above).

Results were plotted as % enzyme activity remaining vs pre-incubation time, and slopes were determined for each inhibitor concentration by linear regression analysis. K_I and k_{inact} values were determined from plots of inverse slope (λ) vs inhibitor concentration.

Allosterism Experiments with Berberine and CYP3A4/5 Enzymes

The allosteric effect of berberine on MDZ metabolism (mediated by either HLMs or CYP3A4 or CYP3A5 Supersomes™) was monitored at eight different substrate concentrations (0 to 250 μM MDZ) and five different inhibitor concentrations (0 to 100 μM berberine). Solutions of berberine and MDZ in 100 mM KP_i buffer, pH 7.4, containing either 0.25 mg/mL HLMs or 2.5 pmols of CYP3A Supersomes™, were pre-equilibrated in a 96-well plate at 37°C/50 rpm in a water bath for three minutes prior to initiating the reactions with the addition of a stock solution of NADPH (pre-warmed to 37°C, 1 mM final concentration). After a three-minute incubation, reactions were quenched with the addition of 20 μL of a 15% aqueous $ZnSO_4$ solution, and 10 pmols of 1'-OH-MDZ-d_4 were added. Protein precipitate was removed by centrifugation, and the supernatants were analyzed by LC-MS/MS.

LC-MS/MS Protocol. LC-MS/MS analyses were conducted on the same Xevo TQ-S Mass Spectrometer (Waters) and ACQUITY UPLC™ system (Waters) described above for the substrate cocktail assay. The Xevo instrument was operated in ESI^+ mode at the same source and desolvation temperatures, and the following mass transitions were monitored in separate ion channels: *m/z* 342 → 324 (1'-OH-MDZ-d_0), *m/z* 346 → 328 (1'-OH-MDZ-d_4) and *m/z* 342 → 234 (4-OH-MDZ). The cone voltage was set to 30 V for all analytes, with collision energies of 35 eV for 1'-OH-MDZ (labeled and unlabeled) and 20 eV for 4-OH-MDZ.

MDZ hydroxylation products from berberine co-incubations were separated on an ACQUITY BEH Phenyl, 1.7 μ, 2.1 x 150 mm, UPLC column (Waters) using a binary solvent gradient (solvent A = 0.1% aqueous formic acid and solvent B = acetonitrile) at a constant flow rate of 0.35 mL/min and a column temperature of 50°C. An isocratic gradient of 25% B was maintained for 5.5 min, then increased

DMD Fast Forward. Published on June 26, 2020 as DOI: 10.1124/dmd.120.091041
This article has not been copyedited and formatted. The final version may differ from this version.

linearly to 95% B over 0.5 min, at which time the gradient was maintained for 1 min prior to column re-equilibration. Under these conditions, 4-OH-MDZ, 1'-OH-MDZ-d_4, 1'-OH-MDZ-d_0, MDZ and berberine had retention times of approximately 3.7, 4.6, 4.7, 5.4 and 6.3 minutes, respectively. Metabolites were quantified through comparison of their peak area ratios (relative to the 1'-OH-MDZ-d_4 peak area) to calibration curves, prepared from synthetic metabolite standards, using linear regression analysis. Limits of quantitation for both metabolites were 20 fmols injected on the column.

Data Analysis

Mass spectral data analyses were conducted using Windows-based Micromass MassLynxNT®, v 4.1, software. GraphPad Prism v7 (GraphPad Software, San Diego, CA) was used to estimate all kinetic parameters using reaction velocities calculated as the mean of duplicate technical replicates. Unless otherwise stated, at least three biological replicates were conducted for all experiments. Goodness-of-fit of the various metabolic/inhibition equations (Michealis-Menten, IC_{50} determination, reversible inhibition, TDI, and substrate inhibition) were evaluated based on visual inspection, the extra sum-of-squares F-test, Akaike information criterion, and randomness of the residuals. Tabulated data are presented as means ± S.D.

Preliminary In Vitro-In Vivo Prediction of Goldenseal-Drug Interactions

A preliminary risk assessment of potential clinical goldenseal-drug interactions due to inhibition of hepatic CYP2C9, CYP2D6 or CYP3A4 activity was made using basic static models (eqs. 1 and 2) (U.S. Food and Drug Administration, 2020). Specifically, the ratios of intrinsic clearance values (R) for a probe drug in the absence to presence of an interacting reversible or time-dependent inhibitor were estimated. Equation 1 predicts the change in clearance due to reversible inhibition:

$$R_1 = 1 + (I_{max,u}/K_{i,u}) \qquad \textit{Equation 1}$$

where $I_{max,u}$ ($I_{max} * f_{u,p}$) is the maximum unbound plasma concentration of the inhibitor (goldenseal alkaloid), and $K_{i,u}$ ($K_i * f_{u,HLM}$) is the experimentally determined reversible inhibition constant

(conservatively estimated as one-half of the IC_{50} value determined in the absence of NADPH in the pre-incubation step, Table 1) corrected for non-specific binding to HLMs ($f_{u,HLM}$). The fraction unbound in plasma ($f_{u,p}$) and $f_{u,HLM}$ (at 0.25 mg/mL microsomal protein) were predicted using GastroPlus® (v9.7, Simulations Plus, Lancaster, CA); values for berberine were 0.75 and 1.0, respectively, and those for hydrastine were 0.10 and 0.79, respectively. I_{max} values were obtained from the literature (1.75 and 470 nM for berberine and hydrastine, respectively; Gupta et al., 2009). Equation 2 predicts the change in probe drug clearance due to TDI:

$$R_2 = \frac{k_{obs} + k_{deg}}{k_{deg}} \qquad \left(k_{obs} = \frac{k_{inact} * 50 * I_{max,u}}{K_{I,u} + (50 * I_{max,u})} \right) \qquad \textit{Equation 2}$$

where $K_{I,u}$ ($K_I * f_{u,HLM}$) and k_{inact} are the TDI binding (corrected for non-specific binding to HLMs) and inactivation rate constants (Table 2), and k_{deg} is the degradation rate constant for a given CYP. For hepatic CYP2C9, CYP2D6 and CYP3A4, k_{deg} has been estimated as 0.00026, 0.000226 and 0.000321 min^{-1}, respectively (Obach et al., 2007).

DMD Fast Forward. Published on June 26, 2020 as DOI: 10.1124/dmd.120.091041
This article has not been copyedited and formatted. The final version may differ from this version.

RESULTS

IC_{50} Shift Experiments: Inhibition of CYP2C9, CYP2D6 and CYP3A4/5 Activities in HLMs by Goldenseal Isoquinoline Alkaloids.

Substrate cocktail assay. Berberine, (-)-β-hydrastine and hydrastinine were tested, by IC_{50} shift assay, as time-dependent inhibitors of CYP2C9, CYP2D6 and CYP3A4/5 activities in HLMs using a cocktail of specific substrate probes. Additionally, tienilic acid (CYP2C9), paroxetine (CYP2D6), and troleandomycin (CYP3A4) were tested as positive controls for clinically relevant isozyme-specific TDI (Bertelsen et al., 2003; McGinnity et al., 2006; Zhao et al., 2005).

Each isoquinoline alkaloid exhibited an IC_{50} shift ratio > 1.5 (the pre-defined cut-off for TDI) for at least one of the CYP activities tested. Berberine had no effect on CYP2C9-mediated diclofenac-4'-hydroxylation (data not shown) but was a relatively strong time-dependent inhibitor of CYP2D6-mediated dextromethorphan *O*-demethylation (Figure 2A) and showed both reversible activation and TDI of CYP3A4/5-mediated MDZ-1'-hydroxylation (Figure 2B). (-)-β-Hydrastine inhibited CYP2C9 (Figure 2C), CYP2D6 (Figure 2D) and CYP3A4/5 (Figure 2E) activities in a time-dependent manner. Hydrastinine had no effect on CYP2C9 or CYP3A4/5 activities (data not shown) but was a moderate time-dependent inhibitor of CYP2D6 (Figure 2F, Table 1).

Cytochrome P450 Kinetic Inactivation by Goldenseal Isoquinoline Alkaloids in HLMs (Determination of K_I and k_{inact}).

TDI experiments were conducted to determine the kinetics of inactivation of CYP2C9, CYP2D6 and CYP3A4/5 activities in HLMs by each alkaloid. The same isozyme-specific substrate probes used in the IC_{50} shift substrate cocktail experiments were used at 10x their reported K_m values (McDonald et al., 2015). (-)-β-Hydrastine was a weak to moderate inactivator of the three enzyme activities (Figure 3, Table 2). Berberine had no effect on CYP2C9 activity (data not shown), was a relatively strong inactivator of CYP2D6, and demonstrated both weak reversible activation and modest TDI of CYP3A4/5

DMD Fast Forward. Published on June 26, 2020 as DOI: 10.1124/dmd.120.091041
This article has not been copyedited and formatted. The final version may differ from this version.

activity (Table 2). Hydrastinine showed moderate TDI of CYP2D6 (Table 2) and had no effect on either CYP2C9 or CYP3A4/5 activity (data not shown).

Preliminary Hepatic CYP-Mediated Goldenseal-Drug Interaction Predictions

The risk of each alkaloid to precipitate clinical pharmacokinetic interactions with drugs metabolized by hepatic CYP2C9, CYP2D6 and CYP3A4/5 was predicted using basic static equations. As reversible inhibitors, the R_1 value for all alkaloids involving all CYP substrates was < 1.02, suggesting low interaction risk. FDA guidance recommends further investigation, either through a clinical study or using mechanistic models, for time-dependent inhibitors with $R_2 \geq 1.25$ (U.S. Food and Drug Administration, 2020). The R_2 values for berberine involving CYP2D6 substrates and for (-)-β-hydrastine involving all CYP substrates exceeded this cut-off; the R_2 for berberine involving TDI of CYP3A4/5 substrates was near the minimum FDA cutoff value (Table 6).

Allosteric Effects of Berberine on CYP3A4/5-Mediated MDZ Metabolism.

Rates of MDZ hydroxylation at both the 1'- and 4-positions, mediated by pooled HLMs (Corning Life Sciences) or recombinant CYP3A4 or CYP3A5 Supersomes™, were monitored across a range of substrate and effector concentrations. A short (3 minute) incubation time was used to minimize CYP3A4/5 enzyme inactivation by berberine. The commercial Ultrapool 150™ HLM preparation contained 57 pmol CYP3A4/mg microsomal protein and 25 pmol/mg CYP3A5 according to Western Blot analysis (Corning).

In the absence of effector, MDZ 1'-hydroxylation showed substrate inhibition kinetics with both HLMs and CYP3A4 Supersomes™. Addition of berberine lowered $K_{i(app)}$ by ~50% with both enzyme sources (i.e. from 900 μM to 420 μM with recombinant CYP3A4, and from 315 μM to 130 μM with HLMs), at which point this binding effect appeared to reach saturation. The addition of high concentrations of berberine (≥ 50 μM) appeared to inhibit MDZ 1'-hydroxylation mediated by recombinant CYP3A4, but not HLMs, causing both an increase in $K_{m(app)}$ and decrease in V_{max} (Figure 4,

DMD Fast Forward. Published on June 26, 2020 as DOI: 10.1124/dmd.120.091041
This article has not been copyedited and formatted. The final version may differ from this version.

Tables 3 and 4). Instead, berberine activated 1'-OH-MDZ formation in HLMs by lowering the $K_{m(app)}$ for MDZ while having no obvious effect on V_{max}. In the absence of effector, the kinetics with CYP3A5 Supersomes™ shifted from substrate inhibition (observed with recombinant CYP3A4) to a simple unienzyme Michaelis-Menten profile. When berberine was added to the CYP3A5 Supersomes™ incubations, an activation effect was observed, due to a lowering of K_m apparent for MDZ (Table 5).

In the absence of effector, the kinetics of 4-OH-MDZ formation in both HLMs and CYP3A4 Supersomes™ were described best by a simple unienzyme Michaelis-Menten model, showing a similar K_m for MDZ (20-25 μM); upon addition of berberine, non-competitive inhibition of MDZ 4-hydroxylation was observed. MDZ 4-hydroxylation by CYP3A5 Supersomes™ also were described best by a simple unienzyme Michaelis-Menten kinetic model, exhibiting a K_m and V_{max} that were both approximately 50% of those for recombinant CYP3A4 (Tables 2-4). When berberine was added to incubations containing CYP3A5 Supersomes™, strong mixed inhibition of MDZ 4-hydroxylation was observed (Figure 5).

In the absence of effector, CYP3A4 Supersomes™ produced a 1'-OH/4-OH-MDZ ratio of 7-9 at the lowest MDZ concentration tested, CYP3A5 Supersomes ™ produced a ratio of 35-40, and HLMs produced a ratio of 10-12. The addition of berberine (up to 100 μM) resulted in a modest increase (1.35 to 1.6-fold) in the maximum metabolite ratio observed for CYP3A4-mediated MDZ hydroxylation, while causing an increase of up to 30-fold in the CYP3A5-mediated metabolite ratio and an increase of 3 to 4-fold in the HLMs-mediated metabolite ratio (Figure 6).

IC_{50} Shift Experiments with CYP3A4/5 Supersomes™: Inhibition of MDZ 1'-Hydroxylation by Berberine and (-)-β-Hydrastine.

Additional studies were conducted to determine the relative ability of berberine and (-)-β-hydrastine to inactivate recombinant CYP3A4 and CYP3A5 separately using MDZ as a probe substrate. The final MDZ concentration in the incubation mixtures was either 2 μM (the reported K_m for CYP3A4)

for experiments involving (-)-β-hydrastine or 20 μM when berberine was used as the inhibitor. In the latter case, the higher concentration of substrate used was an attempt to minimize the observed activation effect of berberine on CYP3A5-mediated MDZ 1'-hydroxylation.

There was essentially no reversible inhibition of CYP3A5-mediated MDZ 1'-hydroxylation by berberine (up to 500 μM) and only weak to moderate TDI (shifted IC_{50} = 83 μM; shift ratio > 6). Berberine was a weak reversible inhibitor of CYP3A4 activity (IC_{50} = ~ 500 μM) but a stronger time-dependent inhibitor of this enzyme (shifted IC_{50} = 9.9 μM; shift ratio = ~50) (Supplemental Figure 1). By contrast, there was no observable difference for the TDI of CYP3A4 vs CYP3A5 by (-)-β-hydrastine (reversible IC_{50} = ~30 μM; shifted IC_{50} = 2.5 μM; shift ratio = 12 for both isozymes) (Supplemental Figure 2).

DISCUSSION

Botanical NP usage continues to increase worldwide as a means to self-treat various illnesses and/or supplement prescribed pharmacotherapeutic regimens (Paine and Roe, 2018; Smith et al., 2019). Co-consuming NPs with prescribed medications can increase the risk of adverse NP-drug interactions, which can lead to suboptimal therapeutic outcomes. Mechanisms of pharmacokinetic NP-drug interactions include inhibition of the CYPs, which are responsible for the metabolic elimination of numerous clinically used drugs, including those with a narrow therapeutic window (Guengerich, 2008; Zanger and Schwab, 2013). Goldenseal is a widely used NP that contains several isoquinoline alkaloids, the most prominent of which are berberine and (-)-β-hydrastine (Weber et al., 2003). Despite clinical studies demonstrating goldenseal or berberine to precipitate pharmacokinetic interactions with the probe substrates MDZ (CYP3A4/5), debrisoquine (CYP2D6), dextromethorphan (CYP2D6), and losartan (CYP2C9) (Gurley et al., 2008a; Gurley et al., 2008b; Guo et al., 2012), a comprehensive characterization of the inhibition kinetics of major isoquinoline alkaloids has not been reported. Robust kinetic parameters are needed to develop PBPK models, which can be used to predict the magnitude and time-course of potential clinical interactions with critical object drugs (i.e., drugs with narrow therapeutic windows), as well as the risk of these interactions in vulnerable populations (e.g., elderly, hepatically-impaired, renally-impaired, pregnant women). Based on these knowledge gaps, the reversible inhibition and TDI kinetics of berberine, (-)-β-hydrastine, and hydrastinine against CYP2C9, CYP2D6, and CYP3A4/5 activities were determined using HLMs.

These isoquinoline alkaloids were predominantly weak reversible inhibitors of the CYP activities tested (at probe substrate concentrations equal to the respective K_m values), generating IC_{50} values in the absence of an NADPH pre-incubation step of >50 μM (a lone exception was berberine, which was a moderate reversible inhibitor of CYP2D6 activity in HLMs, IC_{50} = 9.9 μM) (Table 1). Gupta et al. reported maximum human plasma concentrations of 1.75 and 470 nM, respectively, for berberine and

hydrastine following administration of a single 2.14 g oral dose of a GSE containing 132 mg berberine (6.2% of extract) and 77 mg hydrastine (3.6% of extract) (Gupta et al., 2009). Although no standard dosing protocol exists for GSEs, recommended doses generally range from 250 to 1000 mg 3x daily. The alkaloid percentages contained in the extract used in the Gupta study were within the expected ranges determined for a selection of commercial GSEs (Brown and Roman, 2008). Using these reported I_{max} values for berberine and hydrastine, we conclude that reversible inhibition is an unlikely mechanism of the reported clinical CYP-mediated goldenseal-drug interactions at the level of the liver. However, reversible inhibition of CYP3A4/5 by either alkaloid at the level of the intestine cannot be ruled out based on estimated luminal concentrations ranging from 0.8-1.6 mM (dose/0.25 L per FDA guidance) (U.S. Food and Drug Administration, 2020).

Based on these observations, any clinical NP-drug interaction caused by GSE via inhibition of hepatic CYP2C9, CYP2D6 or CYP3A4/5 metabolism is likely due to TDI of enzyme activity by one or more of the component GSE alkaloids. All of these alkaloids contain a methylenedioxyphenyl ring, a known structural alert for the inactivation of CYP enzymes primarily via formation of metabolic intermediate (MI) complexes (Taxak et al., 2013). MI complexes typically exhibit a distinct absorption maximum at ~455 nm, and evidence for MI complex formation between (-)-β-hydrastine and CYPs 2C9, 2D6 and 3A4 has been described (Chatterjee and Franklin, 2003). It is, therefore, not surprising that we observed TDI of the tested CYPs in HLMs by (-)-β-hydrastine or berberine (Figure 3, Table 2).

Using a basic static model, we predicted clinical goldenseal-drug interactions may result from inactivation of hepatic CYP2C9, CYP2D6 and CYP3A4 by (-)-β-hydrastine and from the inactivation of hepatic CYP2D6 and CYP3A4 by berberine (Table 6). The inactivation parameters used to predict these drug interactions were estimated using a standard Michaelis-Menten model. Recent work by Korzekwa and colleagues suggested that the TDI kinetics of MI complex formation reflects a more complicated 'quasi-irreversible intermediate' model wherein an initial, intermediate, MI complex is reversibly formed and subsequently progresses to an irreversible MI complex (Barnaba, et al., 2016). If the rate at which the

DMD Fast Forward. Published on June 26, 2020 as DOI: 10.1124/dmd.120.091041
This article has not been copyedited and formatted. The final version may differ from this version.

second, irreversible complex forms is significantly slower than the formation rate of the initial complex, estimating TDI kinetics using a Michaelis-Menten model can cause an overprediction of the k_{inact} value, thus resulting in a corresponding overprediction of in vivo drug interaction risk.

Berberine not only showed TDI, but also reversibly activated CYP3A4/5-mediated MDZ 1'-hydroxylation in HLMs. We further evaluated this allosteric relationship by monitoring the effects of berberine on the regiochemistry and kinetics of MDZ hydroxylation by HLMs, and recombinant CYP3A4 and CYP3A5 Supersomes™, using methodology similar to that employed in the study of fluconazole's allosteric effects on MDZ hydroxylation (Yang et al., 2012). Berberine showed weak mixed inhibition along with negative heterotropic cooperativity (lowering $K_{i(app)}$ for substrate inhibition) for MDZ 1'-hydroxylation by CYP3A4 but activated this reaction (lowering $K_{m(app)}$) when catalyzed by CYP3A5. Berberine's allosteric effects on MDZ 1'-hydroxylation in HLMs were an amalgamation of the individual effects observed for recombinant CYP3A4 and CYP3A5, exhibiting positive and negative heterotropic cooperativity via lowering of both $K_{m(app)}$ and $K_{i(app)}$. Berberine acted as a non-competitive inhibitor of MDZ 4-hydroxylation by both HLMs and recombinant CYP3A4 but was a mixed inhibitor of this reaction when catalyzed by CYP3A5. The berberine effect on CYP3A4 kinetics for this reaction was dominant in HLMs because, based on relative intrinsic clearance rates (Tables 4, 5), the alkaloid was a stronger inhibitor of MDZ 4-hydroxylation by CYP3A5.

The differences in MDZ metabolic kinetics between CYP3A4 and CYP3A5 resulted in large variability in the maximum MDZ 1'-OH/4-OH ratios produced by the two isozymes. In the absence of effector, CYP3A4 produced a maximum observed metabolite ratio of ~8, while that produced by CYP3A5 was ~5-fold higher (the ratio decreased substantively as MDZ concentrations approached and surpassed the K_m for 4-hydroxylation). Adding berberine increased the ratio produced by all three enzyme sources, albeit to different degrees. Because berberine inhibited CYP3A4-mediated MDZ hydroxylation at both the 1' and 4 positions, a relatively modest increase (~1.4-fold) was observed in the maximum metabolite ratio. In contrast, berberine not only activated CYP3A5-mediated MDZ 1'-

DMD Fast Forward. Published on June 26, 2020 as DOI: 10.1124/dmd.120.091041
This article has not been copyedited and formatted. The final version may differ from this version.

hydroxylation, but more strongly inhibited MDZ 4-hydroxylation. This synergistic effect led to more than a 30-fold increase in the observed ratio produced by CYP3A5. As expected, the 3 to 4-fold increase in MDZ metabolite ratio effected by berberine in HLMs (which contain both CYP3A4 and CYP3A5) lay between the values observed for the individual isozymes. In a similar experiment, fluconazole decreased the maximum MDZ metabolite ratio produced by recombinant CYP3A4 by >50%, as it more strongly inhibited hydroxylation at the 1' position of MDZ compared to the 4 position (Yang et al., 2012).

These allosteric data highlight a potential issue with using MDZ 1'-hydroxylation as a probe to monitor the effect of berberine or GSE on CYP3A4/5 activity in vivo. Because berberine is a stronger time-dependent inhibitor of CYP3A4 (IC_{50} shift ratio ~50) compared to CYP3A5 (shift ratio ~6), the possibility exists, especially after prolonged treatment with the alkaloid, that activation of CYP3A5-mediated MDZ 1'-hydroxylation could mask some degree of CYP3A4 inactivation. Therefore, if MDZ is used as an in vivo CYP3A4/5 probe in clinical studies involving GSE or berberine, monitoring MDZ 4-hydroxylation should be considered, as an increase over control in the MDZ 1'-OH/4-OH metabolite ratio would suggest an increased involvement of CYP3A5 in MDZ metabolism.

Small structural differences between CYP3A4 and CYP3A5 cause a marked alteration in how each isozyme binds to berberine which, in turn, leads to the observed opposing allosteric interactions on MDZ hydroxylation effected by the alkaloid. We propose that berberine may activate MDZ 1'-hydroxylation by CYP3A5 through occupation of the peripheral allosteric site most often associated with progesterone binding (Williams et al., 2004). Berberine is similar in size and overall structure to progesterone (Figure 1), a steroid known to promote metabolism of several different CYP3A4/5 probe substrates (Niwa et al., 2003; Polic and Auclair, 2017). In a similar fashion to the berberine activation reported here, progesterone increased CYP3A4/5-mediated nifedipine oxidation in HLMs by lowering $K_{m(app)}$ while having no effect on V_{max} (Niwa et al., 2003). We postulate that berberine binds more strongly to the progesterone site of CYP3A5 but preferentially binds within the active site of CYP3A4, leading to negative heterotropic cooperativity with MDZ along with increased mechanism-based

DMD Fast Forward. Published on June 26, 2020 as DOI: 10.1124/dmd.120.091041
This article has not been copyedited and formatted. The final version may differ from this version.

inactivation of that enzyme. Given the report of a (ritonavir bound) CYP3A5 x-ray crystal structure (Hsu et al., 2018), testing this theory through a docking site comparison of berberine within the CYP3A4 and CYP3A5 active and peripheral binding sites is warranted.

TDI of metabolic drug elimination has clinical implications for the management of drug therapies. Both the onset and offset of the inhibitory effect must be fully characterized to anticipate when and by how much an object drug dose should be adjusted. This scenario is most relevant for narrow therapeutic window drugs such as the calcineurin inhibitors, which are metabolized by CYP3A4/5 (Hesselink et al., 2005), and several antidepressants that are metabolized by CYP2D6 (Kwadijk-de Gijsel et al., 2009). While inactivation of CYP enzymes might occur rapidly under optimal conditions, a return to the original uninhibited state will take days because of its dependence on the half-life of the CYP enzyme (~24-48 hr). The K_I and k_{inact} values generated in this study can be used, in conjunction with expected concentration-time profiles of inhibitor at the site(s) of metabolism, to simulate the time-course of enzyme inactivation and changes in substrate exposure in blood using PBPK modeling and inform the clinical dosing decision process.

In summary, we report robust kinetic parameters for the reversible inhibition and TDI of CYP2C9, CYP2D6 and CYP3A4/5 activities in HLMs by the goldenseal component isoquinoline alkaloids berberine, (-)-β-hydrastine and hydrastinine. These data are a necessary precursor to the development of a PBPK model that can be used to predict potential adverse clinical NP-drug interactions resulting from inhibition of CYP metabolism by goldenseal. We also investigated the allosteric interactions observed with berberine on CYP3A4/5 activity, with the alkaloid exhibiting isozyme-specific positive (CYP3A5) and negative (CYP3A4) heterotropic cooperativity with respect to MDZ 1'-hydroxylation. These complex interactions should be considered in the design and analysis of future clinical studies that monitor the effect of berberine or goldenseal on CYP3A4/5-mediated drug metabolism.

Acknowledgements

The authors would like to thank James Nguyen, with the Department of Pharmaceutical Sciences at Washington State University, for his valuable contributions in predicting the fraction unbound values for the goldenseal alkaloids.

Authorship Contributions

Participated in research design: Tian, Thummel, Paine, Rettie, and McDonald

Conducted experiments: McDonald

Contributed new reagents or analytic tools: N/A

Performed data analysis: McDonald

Wrote or contributed to the writing of the manuscript: Tian, Thummel, Paine, Rettie, and McDonald

REFERENCES

Asher GN, Corbett AH, and Hawke RL (2017) Common herbal dietary supplement-drug interactions. *Am Fam Physician* **96:**101-107.

Bertelsen KM, Venkatakrishnan K, Von Moltke LL, Obach RS, and Greenblat DJ (2003) Apparent mechanism-based inhibition of human CYP2D6 in vitro by paroxetine: comparison with fluoxetine and quinidine. *Drug Metab Dispos* **31**:289-293.

Brown PN, and Roman MC (2008) Determination of hydrastine and berberine in goldenseal raw materials, extracts and dietary supplements by high-performance liquid chromatography with UV: collaborative study. *JAOAC Int.* **91**:694-701.

Budzinski JW, Foster BC, Vandenhoek S, and Arnason JT (2000) An in vitro evaluation of human cytochrome P450 3A4 inhibition by selected commercial herbal extracts and tinctures. *Phytomedicine* **7:**273-282.

Chatterjee P and Franklin MR (2003) Human cytochrome P450 inhibition and metabolic-intermediate complex formation by goldenseal extract and its methylenedioxyphenyl components. *Drug Metab Dispos* **31:**1391-1397.

Etheridge AS, Black SR, Patel PR, So J, and Mathews JM (2007) An in vitro evaluation of cytochrome P450 inhibition and P-glycoprotein interaction with goldenseal, Ginkgo biloba, grape seed, milk thistle, and ginseng extracts and their constituents. *Planta Med* **73:**731-741.

Ettefagh KA, Burns JT, Junio HA, Kaatz GW, and Cech NB (2011) Goldenseal (*Hydrastis canadensis* L.) extracts synergistically enhance the antibacterial activity of berberine via efflux pump inhibition. *Planta Med* **77:**835-840.

Foster BC, Vandenhoek S, Hana J, Krantis A, Akhtar MH, Bryan M, Budzinski JW, Ramputh A, and Arnason JT (2003) In vitro inhibition of human cytochrome P450-mediated metabolism of marker substrates by natural products. *Phytomedicine* **10:**334-342.

Guengerich FP (2008) Cytochrome P450 and chemical toxicology. *Chem Res Toxicol* **21:**70-83.

Guo Y, Chen Y, Tan ZR, Klaassen CD, and Zhou HH (2012) Repeated administration of berberine inhibits cytochromes P450 in humans. *Eur J Clin Pharmacol* **68:**213-217.

Gupta PK, Barone G, Gurley BJ, Fifer EK, and Hendrickson HP (2015) Hydrastine pharmacokinetics and metabolism after a single oral dose of goldenseal (*Hydrastis canadensis*) to humans. *Drug Metab Dispos* **43:**534-552.

Gupta PK, Hubbard M, Gurley B, and Hendrickson HP (2009) Validation of a liquid chromatography-tandem mass spectrometric assay for the quantitative determination of hydrastine and berberine in human serum. *J Pharm Biomed Anal* **49:**1021-1026.

Gurley BJ, Swain A, Hubbard MA, Hartsfield F, Thaden J, Williams DK, Gentry WB, and Tong Y (2008a) Supplementation with goldenseal (*Hydrastis canadensis*), but not kava kava (*Piper methysticum*), inhibits human CYP3A activity in vivo. *Clin Pharmacol Ther* **83:**61-69.

Gurley BJ, Swain A, Hubbard MA, Williams DK, Barone G, Hartsfield F, Tong Y, Carrier DJ, Cheboyina S, and Battu SK (2008b) Clinical assessment of CYP2D6-mediated herb-drug interactions in humans: effects of milk thistle, black cohosh, goldenseal, kava kava, St. John's wort, and Echinacea. *Mol Nutr Food Res* **52:**755-763.

Hermann R and von Richter O (2012) Clinical evidence of herbal drugs as perpetrators of pharmacokinetic drug interactions. *Planta Med* **78:**1458-1477.

Hesselink DA, van Gelder T, and van Schaik RH (2005) The pharmacogenetics of calcineurin inhibitors: one step closer toward individualized immunosuppression? *Pharmacogenomics* **6:**323-337.

Hsu MH, Savas U, and Johnson EF (2018) The x-ray crystal structure of the human mono-oxygenase cytochrome P450 3A5-ritonavir complex reveals active site differences between P450s 3A4 and 3A5. *Mol Pharmacol* **93:**14-24.

Kellogg JJ, Paine MF, McCune JS, Oberlies NH, and Cech NB (2019) Selection and characterization of botanical natural products for research studies: a NaPDI center recommended approach. *Nat Prod Rep* **36:**1196-1221.

Kwadijk-de Gijsel S, Bijl MJ, Visser LE, van Schaik RHN, Hofman A, Vulto AG, van Gelder T, and Ch. Stricker BH (2009) Variations in the CYP2D6 gene is associated with a lower serum sodium concentration in patients on antidepressants. *British Journal of Clinical Pharmacology* **68:**221-225.

Lo SN, Chang YP, Tsai KC, Chang CY, Wu TS, and Ueng YF (2013) Inhibition of CYP1 by berberine, palmatine, and jatrorrhizine: selectivity, kinetic characterization, and molecular modeling. *Toxicol Appl Pharmacol* **272:**671-680.

McDonald MG, Au NT, and Rettie AE (2015) P450-based drug-drug interactions of amiodarone and its metabolites: diversity of inhibitory mechanisms. *Drug Metab Dispos* **43:**1661-1669.

McGinnity DF, Berry AJ, Kenny JR, Grime K, and Riley RJ (2006) Evaluation of time-dependent cytochrome P450 inhibition using cultured human hepatocytes. *Drug Metab Dispos* **34**:1291-1300.

Niwa T, Shiraga T, Yamasaki S, Ishibashi K, Ohno Y, and Kagayama A (2003) In vitro activation of 7-benzyloxyresorufin O-debenzylation and nifedipine oxidation in human liver microsomes. *Xenobiotica* **33:**717-729.

Obach RS, Walsky RL, and Venkatakrishnan K (2007) Mechanism-based inactivation of human cytochrome P450 enzymes and the prediction of drug-drug interactions. *Drug Metab Dispos* **35**:246-255.

Paine MF, Shen DD, and McCune JS (2018) Recommended approaches for pharmacokinetic natural product-drug interaction research: a NaPDI Center commentary. *Drug Metab Dispos* **46:**1041-1045.

Paine MF, and Roe AL (2018) "Green medicine": the past, present and future of botanicals. *Clin Pharmacol Ther* **104**:410-415.

Polic V and Auclair K (2017) Allosteric activation of cytochrome P450 3A4 via progesterone bioconjugation. *Bioconjug Chem* **28:**885-889.

Raner GM, Cornelious S, Moulick K, Wang Y, Mortenson A, and Cech NB (2007) Effects of herbal products and their constituents on human cytochrome P450(2E1) activity. *Food Chem Toxicol* **45:**2359-2365.

Sadeque AJ, Eddy AC, Meier GP, and Rettie AE (1992) Stereoselective sulfoxidation by human flavin-containing monooxygenase. Evidence for catalytic diversity between hepatic, renal, and fetal forms. *Drug Metab Dispos* **20:**832-839.

Smith T, Gillespie M, Eckl V, Knepper J, and Morton Reynolds C (2019) Market report: herbal supplement sales increase by 9.4% in 2018. *Herbalgram***:**62-73.

Taxak N, Patel B, and Bharatam PV (2013) Carbene generation by cytochromes and electronic structure of heme-iron-porphyrin-carbene complex: a quantum chemical study. *Inorg Chem* **52:**5097-5109.

U.S. Food and Drug Administration (2020) In vitro drug interaction studies - cytochrome P450 enzyme- and transporter-mediated drug interactions: guidance for industry.

Weber HA, Zart MK, Hodges AE, Molloy HM, O'Brien BM, Moody LA, Clark AP, Harris RK, Overstreet JD, and Smith CS (2003) Chemical comparison of goldenseal (*Hydrastis canadensis* L.) root powder from three commercial suppliers. *J Agric Food Chem* **51:**7352-7358.

Williams PA, Cosme J, Vinkovic DM, Ward A, Angove HC, Day PJ, Vonrhein C, Tickle IJ, and Jhoti H (2004) Crystal structures of human cytochrome P450 3A4 bound to metyrapone and progesterone. *Science* **305:**683-686.

Wu X, Li Q, Xin H, Yu A, and Zhong M (2005) Effects of berberine on the blood concentration of cyclosporin A in renal transplanted recipients: clinical and pharmacokinetic study. *Eur J Clin Pharmacol* **61:**567-572.

Yang J, Atkins WM, Isoherranen N, Paine MF, and Thummel KE (2012) Evidence of CYP3A allosterism in vivo: analysis of interaction between fluconazole and midazolam. *Clin Pharmacol Ther* **91:**442-449.

Zanger UM and Schwab M (2013) Cytochrome P450 enzymes in drug metabolism: regulation of gene expression, enzyme activities, and impact of genetic variation. *Pharmacol Ther* **138:**103-141.

Zhao P, Kunze KL, and Lee CA (2005) Evaluation of time-dependent inactivation of CYP3A in cryopreserved human hepatocytes. *Drug Metab Dispos* **33**:853-861.

Zhao Y, Hellum BH, Liang A, and Nilsen OG (2015) Inhibitory mechanisms of human CYPs by three alkaloids isolated from traditional Chinese herbs. *Phytother Res* **29:**825-834.

FOOTNOTES

a. This work was supported by the National Institutes of Health National Center for Complimentary and Integrative Health [Grant U54 AT008909]. The content is solely the responsibility of the authors and does not necessarily represent the official views of the NIH.

b. Reprint requests:

Matthew G. McDonald, Ph.D.

Department of Medicinal Chemistry

University of Washington, Box 357610

1959 NE Pacific, Seattle WA 98195

Telephone: (206) 384-3386

Fax: (206) 685-3252

Email: mcmatt@uw.edu

c. [1]Current address: Drug Disposition, Eli Lilly and Company, Indianapolis, Indiana, USA

DMD Fast Forward. Published on June 26, 2020 as DOI: 10.1124/dmd.120.091041
This article has not been copyedited and formatted. The final version may differ from this version.

FIGURE LEGENDS

Figure 1. Structures of A) major isoquinoline alkaloids isolated from goldenseal (*Hydrastis canadensis* L. (Ranunculaceae)) extract and B) the steroid progesterone.

Figure 2. Results from IC_{50} shift experiments showing TDI of A) CYP2D6-mediated dextromethorphan *O*-demethylation by berberine, B) CYP3A4/5-mediated MDZ 1'-hydroxylation by berberine, C) CYP2C9-mediated diclofenac 4'-hydroxylation by (-)-β-hydrastine, D) CYP2D6-mediated dextromethorphan *O*-demethylation by (-)-β-hydrastine, E) CYP3A4/5-mediated MDZ 1'-hydroxylation by (-)-β-hydrastine and F) CYP2D6-mediated dextromethorphan *O*-demethylation by hydrastinine, in HLMs. Mean IC_{50} values for each set of experiments (repeated in triplicate) are shown in Table 1.

Figure 3. CYP inactivation kinetics showing inhibition of A) CYP2C9-mediated diclofenac 4'-hydroxylation by (-)-β-hydrastine, B) CYP2D6-mediated dextromethorphan *O*-demethylation by (-)-β-hydrastine, C) CYP3A4/5-mediated MDZ 1'-hydroxylation by (-)-β-hydrastine, D) CYP2D6-mediated dextromethorphan *O*-demethylation by berberine, E) CYP3A4/5-mediated MDZ 1'-hydroxylation by berberine and F) CYP2D6-mediated dextromethorphan *O*-demethylation by hydrastinine in HLMs as a function of enzyme/NADPH pre-incubation time. K_I and k_{inact} values (see Table 2) were determined from plots (shown as insets in graphs A-F) of inverse slope (λ), for the individual lines in each graph, vs inhibitor concentration. *Berb*, Berberine.

Figure 4. Plots showing allosteric effects of berberine on the kinetics of MDZ 1'-hydroxylation mediated by HLMs or CYP3A4 or CYP3A5 Supersomes™. With both HLMs and CYP3A4 Supersomes™, the kinetics were consistent with a substrate inhibition model, with an inhibitory allosteric effect exhibited upon the addition of berberine (i.e., decreased K_i). There also appears to be some mixed inhibition of CYP3A4 at high berberine concentrations. In contrast, the kinetics of MDZ 1'-hydroxylation by CYP3A5 were described best by a simple, unienzyme Michaelis-Menten model. Berberine activated MDZ 1'-hydroxylation in both HLMs and CYP3A5 Supersomes™ by lowering $K_{m(app)}$ (Tables 2-4).

Figure 5. The kinetics of MDZ 4-hydroxylation, by HLMs or by recombinant CYP3A4 or CYP3A5 Supersomes™, were described best by a simple, unienzyme Michaelis-Menten model. Berberine acted as a non-competitive inhibitor of CYP3A4 and HLMs-mediated MDZ 4-hydroxylation and a mixed inhibitor of this reaction when catalyzed by CYP3A5 (Tables 2-4).

Figure 6. Effect of berberine on the metabolite ratio for MDZ hydroxylation (i.e. 1'-OH/4-OH-MDZ) produced by HLMs or CYP3A4 or CYP3A5 Supersomes™. Metabolite ratios were highest at the lowest concentrations of substrate tested and decreased markedly at concentrations exceeding the K_m for MDZ 4-hydroxylation (~12-25 μM). When berberine was added as effector, an increase in the maximum metabolite ratio was observed with all three enzyme sources; however, this increase was modest for CYP3A4 (1.35 to 1.6-fold at 100 μM berberine) compared to CYP3A5 (~30-fold), while the 3.5-fold increase in the maximum metabolite ratio produced by berberine in HLMs lay in between these values.

DMD Fast Forward. Published on June 26, 2020 as DOI: 10.1124/dmd.120.091041
This article has not been copyedited and formatted. The final version may differ from this version.

Table 1. Results of IC_{50} shift experiments showing TDI of CYP2C9, CYP2D6 and CYP3A4/5 activities in HLMs by goldenseal component alkaloids.

Inhibitor	Probe Substrate	Inhibited Enzyme	IC_{50} (μM)[a]		Shift Ratio[b]
			(-) NADPH	(+) NADPH	
Berberine	Dextromethorphan	CYP2D6	9.9 ± 1.3	1.6 ± 0.3	6.0
Berberine	MDZ	CYP3A4/5	Activation	180 ± 25	-
(-)-β-Hydrastine	Diclofenac	CYP2C9	120 ± 30	31 ± 3.2	3.9
(-)-β-Hydrastine	Dextromethorphan	CYP2D6	270 ± 21	80 ± 18	3.4
(-)-β-Hydrastine	MDZ	CYP3A4/5	58 ± 7.6	9.9 ± 1.5	5.9
Hydrastinine	Dextromethorphan	CYP2D6	65 ± 21	8.4 ± 1.1	7.7
Tienilic Acid	Diclofenac	CYP2C9	2.8	0.2	13
Paroxetine	Dextromethorphan	CYP2D6	0.9	0.1	9
Troleandomycin	MDZ	CYP3A4/5	61	1.5	40

[a]Prior to the addition of substrate, HLMs were pre-incubated with inhibitor for 30 minutes in the presence (+) or absence (-) of NADPH cofactor.

[b]Shift Ratio = IC_{50} (-) NADPH/IC_{50} (+) NADPH

Values denote means ± S.D. of 3 separate experiments with the exception of the tienilic acid, paroxetine and troleandomycin inhibitors, which were each run as a singlet. These three compounds were chosen as positive controls for the IC_{50} shift experiments because they are known to exhibit strong isozyme-specific TDI of CYP2C9, CYP2D6 and CYP3A4/5 activities, respectively. *MDZ*, midazolam.

DMD Fast Forward. Published on June 26, 2020 as DOI: 10.1124/dmd.120.091041
This article has not been copyedited and formatted. The final version may differ from this version.

Table 2. Kinetic parameters for the inactivation of CYP2C9, CYP2D6 and CYP3A4/5 in HLMs by goldenseal component alkaloids.

Inhibitor	Inhibited Enzyme	K_I (μM)	k_{inact} (min^{-1})	k_{inact}/K_I[a] ($mM^{-1}min^{-1}$)
Berberine	CYP2D6	2.68 ± 0.26	0.065 ± 0.006	24.3
Berberine	CYP3A4/5	14.8 ± 2.6	0.019 ± 0.005	1.3
(-)-β-Hydrastine	CYP2C9	49 ± 16	0.036 ± 0.007	0.7
(-)-β-Hydrastine	CYP2D6	> 250	> 0.06	< 0.2
(-)-β-Hydrastine	CYP3A4/5	28 ± 12	0.056 ± 0.005	2.0
Hydrastinine	CYP2D6	37 ± 13	0.049 ± 0.009	3.8

Values denote means ± S.D. of 3 separate experiments.

[a]Reported k_{inact}/K_I values ($mM^{-1}min^{-1}$) for the TDI of specific CYP activities, in either HLMs (paroxetine, troleandomycin) or human hepatocytes (tienilic acid), for clinically relevant time-dependent inhibitors: tienilic acid (CYP2C9) = 25; paroxetine (CYP2D6) = 35; troleandomycin (CYP3A4/5) = 13.3 (Bertelsen et al., 2003; McGinnity et al., 2006; Zhao et al., 2005).

DMD Fast Forward. Published on June 26, 2020 as DOI: 10.1124/dmd.120.091041
This article has not been copyedited and formatted. The final version may differ from this version.

Table 3. Allosteric effects of berberine on MDZ hydroxylation in HLMs.

Berberine (μM)	1'-Hydroxy MDZ				4-Hydroxy MDZ		
	K_m[a]	V_{max}[a]	V_{max}/K_m[a]	K_i[a]	K_m[a]	V_{max}[a]	V_{max}/K_m[a]
0	2.29 ± 0.29	2110 ± 380	930 ± 220	315 ± 92	21.1 ± 4.4	1260 ± 220	60.8 ± 9.4
5	1.63 ± 0.41	2080 ± 380	1330 ± 370	301 ± 86	25.3 ± 6.2	1150 ± 230	48.3 ± 16.5
25	1.58 ± 0.12	2280 ± 330	1450 ± 210	202 ± 28	26.6 ± 4.5	960 ± 180	37.1 ± 10.1
50	1.22 ± 0.18	2010 ± 220	1680 ± 300	156 ± 17	28.8 ± 6.5	680 ± 130	26.6 ± 7.9
100	1.06 ± 0.15	1880 ± 120	1810 ± 310	130 ± 17	23.2 ± 4.3	450 ± 60	20.0 ± 3.6

[a]Units: K_m and K_i are given in μM; V_{max} is in pmol/min/mg microsomal protein; V_{max}/K_m is in μL/min/mg protein.

Values denote means ± S.D. of 4 separate experiments. *MDZ*, midazolam

Table 4. Allosteric effects of berberine on MDZ hydroxylation by recombinant CYP3A4.

Berberine (μM)	1'-Hydroxy MDZ				4-Hydroxy MDZ		
	K_m[a]	V_{max}[a]	V_{max}/K_m[a]	K_i[a]	K_m[a]	V_{max}[a]	V_{max}/K_m[a]
0	1.38 ± 0.22	28.0 ± 4.6	20.7 ± 4.1	900 ± 250	25.0 ± 6.9	26.4 ± 7.5	1.13 ± 0.40
5	1.28 ± 0.25	31.3 ± 3.7	24.7 ± 2.6	610 ± 190	27.4 ± 8.9	27.1 ± 5.5	1.05 ± 0.29
25	1.34 ± 0.20	24.7 ± 4.0	18.6 ± 2.9	560 ± 120	40.1 ± 17	19.5 ± 6.3	0.56 ± 0.25
50	1.63 ± 0.39	23.4 ± 2.6	15.2 ± 4.9	420 ± 160	30.0 ± 3.4	14.6 ± 5.4	0.50 ± 0.20
100	2.04 ± 0.55	21.4 ± 2.4	11.0 ± 2.7	470 ± 70	32.0 ± 6.2	11.5 ± 4.2	0.37 ± 0.13

[a]Units: K_m and K_i are given in μM; V_{max} is in pmol/min/pmol CYP3A4; V_{max}/K_m is in μL/min/pmol CYP3A4.

Values denote means ± S.D. of 4 separate experiments. *MDZ*, midazolam

DMD Fast Forward. Published on June 26, 2020 as DOI: 10.1124/dmd.120.091041
This article has not been copyedited and formatted. The final version may differ from this version.

Table 5. Allosteric effects of berberine on MDZ hydroxylation by recombinant CYP3A5.

Berberine (μM)	1'-Hydroxy MDZ			4-Hydroxy MDZ		
	K_m[a]	V_{max}[a]	V_{max}/K_m[a]	K_m[a]	V_{max}[a]	V_{max}/K_m[a]
0	1.55 ± 0.18	59.3 ± 12.5	38.5 ± 12.9	12.6 ± 2.7	14.9 ± 2.6	1.20 ± 0.09
5	1.55 ± 0.50	58.7 ± 8.9	41.6 ± 19.3	20.5 ± 4.1	14.1 ± 2.3	0.69 ± 0.07
25	1.11 ± 0.10	58.2 ± 14.3	51.5 ± 9.7	39.4 ± 4.9	12.4 ± 2.1	0.32 ± 0.09
50	1.01 ± 0.15	56.3 ± 12.1	54.7 ± 10.8	60.5 ± 5.8	11.4 ± 2.8	0.19 ± 0.05
100	0.91 ± 0.11	53.9 ± 11.5	58.9 ± 15.4	100 ± 28	10.0 ± 3.3	0.10 ± 0.02

[a]Units: K_m and K_i are given in μM; V_{max} is in pmol/min/pmol CYP3A5; V_{max}/K_m is in μL/min/pmol CYP3A5

Values denote means ± S.D. of 3 separate experiments. *MDZ*, midazolam

DMD Fast Forward. Published on June 26, 2020 as DOI: 10.1124/dmd.120.091041
This article has not been copyedited and formatted. The final version may differ from this version.

Table 6. Preliminary Hepatic CYP-Mediated Goldenseal-Drug Interaction Predictions.

Inhibitor	R_2 Value		
	CYP2C9	**CYP2D6**	**CYP3A4**
Berberine	1.00	7.90	1.26
(-)-β-Hydrastine	8.94	~4	17.8

R_2 represents the ratio of intrinsic clearance values for a probe drug in the absence to presence of an interacting time-dependent CYP inhibitor (predicted using a basic static model; U.S. Food and Drug Administration, 2020).

DMD Fast Forward. Published on June 26, 2020 as DOI: 10.1124/dmd.120.091041
This article has not been copyedited and formatted. The final version may differ from this version.

Figure 1

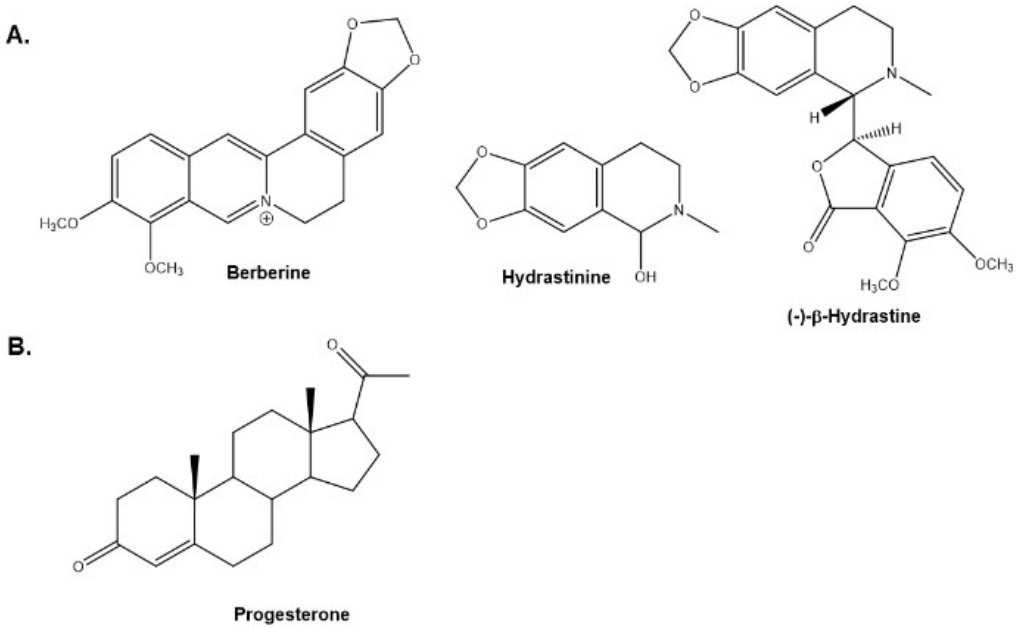

DMD Fast Forward. Published on June 26, 2020 as DOI: 10.1124/dmd.120.091041
This article has not been copyedited and formatted. The final version may differ from this version.

Figure 2

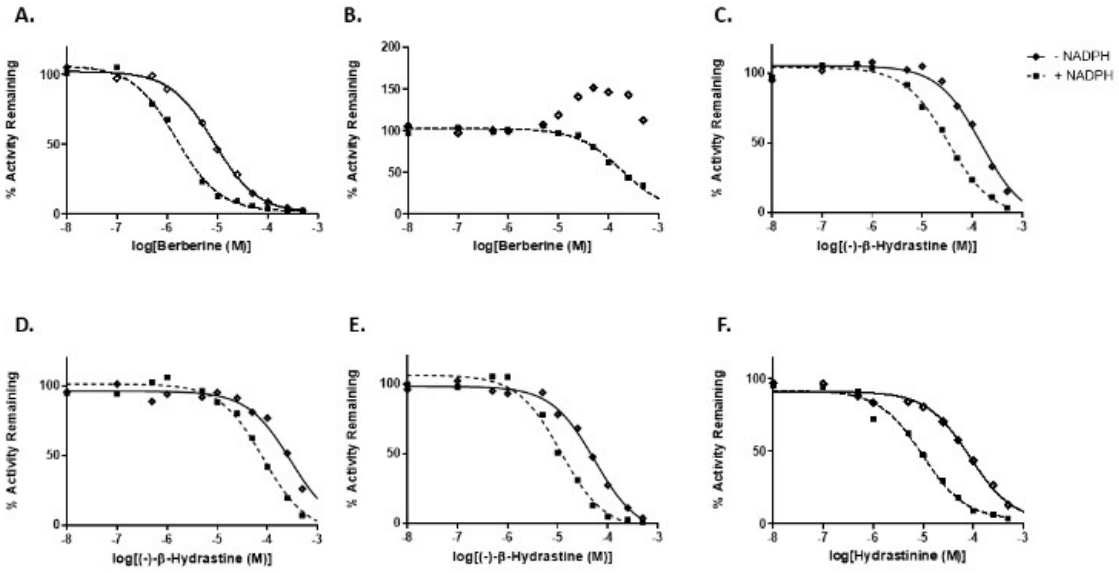

DMD Fast Forward. Published on June 26, 2020 as DOI: 10.1124/dmd.120.091041
This article has not been copyedited and formatted. The final version may differ from this version.

Figure 3.

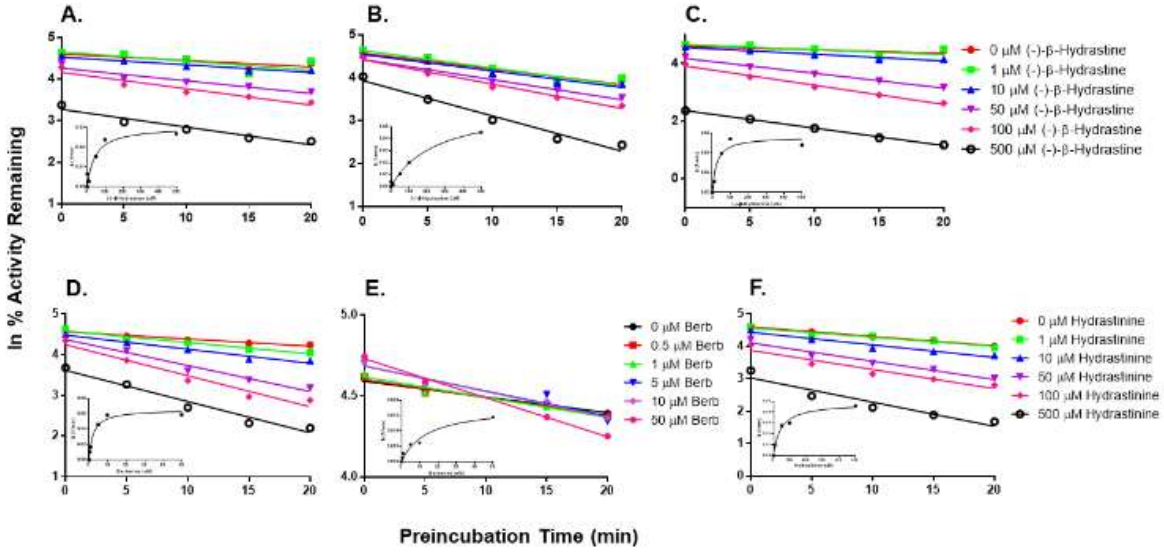

DMD Fast Forward. Published on June 26, 2020 as DOI: 10.1124/dmd.120.091041
This article has not been copyedited and formatted. The final version may differ from this version.

Figure 4

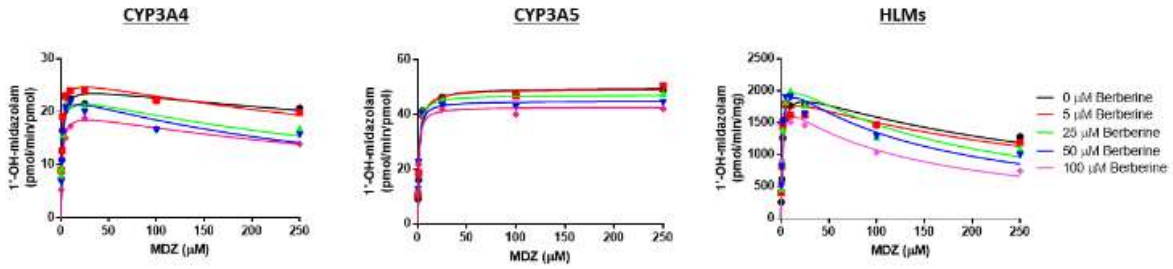

DMD Fast Forward. Published on June 26, 2020 as DOI: 10.1124/dmd.120.091041
This article has not been copyedited and formatted. The final version may differ from this version.

Figure 5

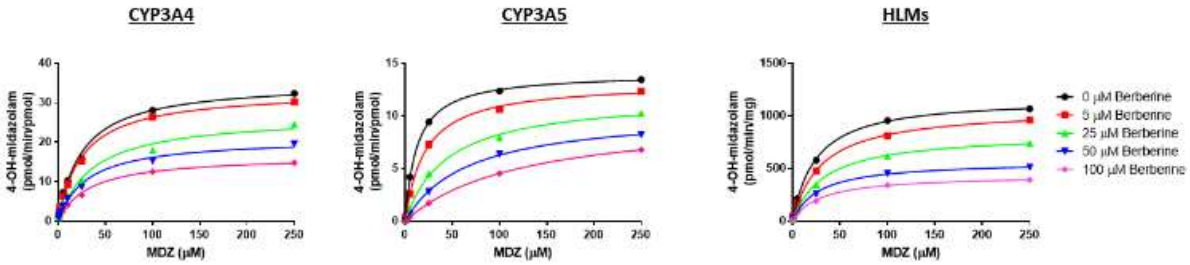

DMD Fast Forward. Published on June 26, 2020 as DOI: 10.1124/dmd.120.091041
This article has not been copyedited and formatted. The final version may differ from this version.

Figure 6

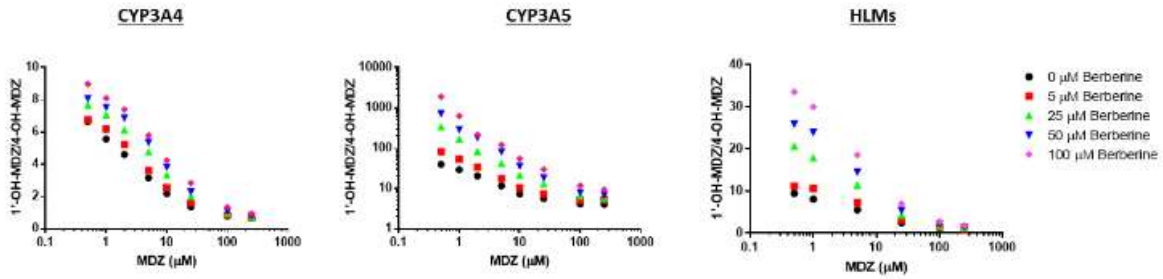

SUPPLEMENTAL MATERIALS

Submitted for publication in *Drug Metabolism and Disposition*

Modulation of Major Human Liver Microsomal Cytochromes P450 by Component Alkaloids of Goldenseal: Time-Dependent Inhibition and Allosteric Effects

Matthew G. McDonald, Dan-Dan Tian[1], Kenneth E. Thummel, Mary F. Paine, Allan E. Rettie

Supplemental Figure 1. IC_{50} shift experiments with berberine, showing TDI of recombinant CYP3A4 or CYP3A5-mediated MDZ 1'-hydroxylation. Data shown are mean values determined from two technical replicates at each inhibitor concentration. TDI of CYP3A4 (reversible IC_{50} = ~500 μM; shifted IC_{50} = 9.9 μM; shift ratio ~50), and CYP3A5 (reversible IC_{50} > 500 μM; shifted IC_{50} = 83 μM; shift ratio > 6) mediated MDZ 1'-hydroxylation by berberine.

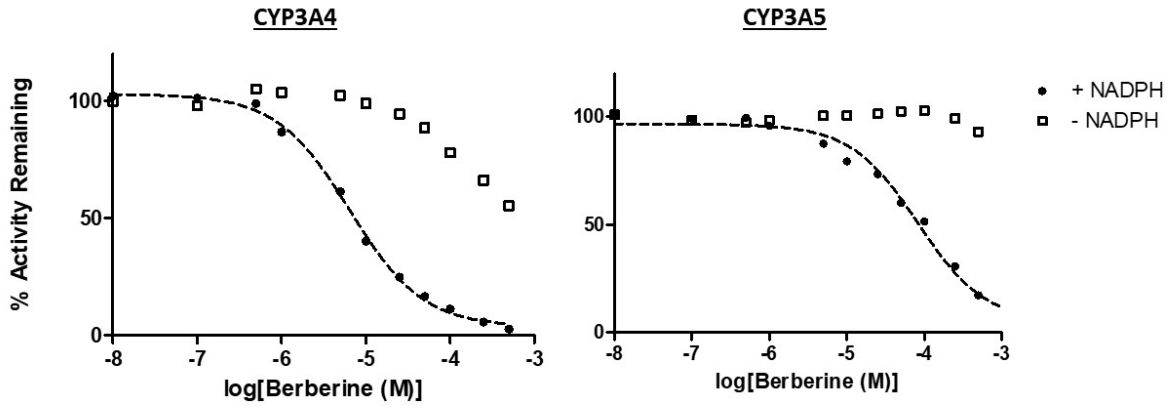

Supplemental Figure 2. IC_{50} shift experiments, with (-)-β-hydrastine, showing TDI of recombinant CYP3A4 or CYP3A5-mediated MDZ 1'-Hydroxylation. Data shown are mean values determined from two technical replicates at each inhibitor concentration. Reversible IC_{50} = ~30 μM; shifted IC_{50} = 2.5 μM; shift ratio = 12 for the inhibition of both CYP3A4- and CYP3A5-mediated MDZ 1'-hydroxylation by (-)-β-hydrastine.